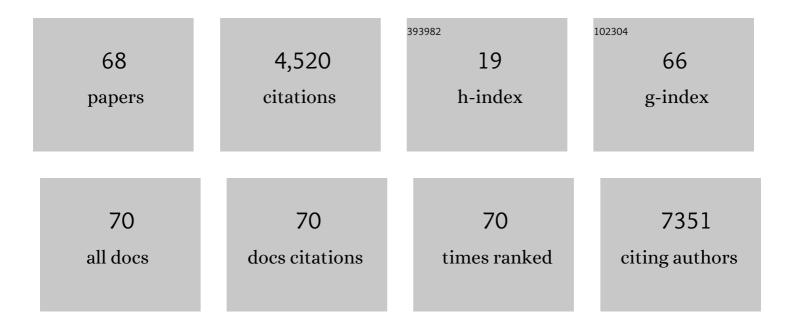
List of Publications by Year in descending order

Source: https://exaly.com/author-pdf/4863065/publications.pdf Version: 2024-02-01



SHAONING YU

#	Article	IF	CITATIONS
1	Rapid identification of bacterial mixtures in urine using MALDI-TOF MS-based algorithm profiling coupled with magnetic enrichment. Analyst, The, 2022, 147, 443-449.	1.7	8
2	Highly efficient synergistic biocatalysis driven by stably loaded enzymes within hierarchically porous iron/cobalt metal–organic framework <i>via</i> biomimetic mineralization. Journal of Materials Chemistry B, 2022, 10, 1553-1560.	2.9	15
3	Enzyme-assisted ReMALDI-MS assay for quantification of cholesterol in food. Food Chemistry, 2022, 383, 132444.	4.2	2
4	A versatile biomimetic multienzyme cascade nanoplatform based on boronic acid-modified metal–organic framework for colorimetric biosensing. Journal of Materials Chemistry B, 2022, 10, 3444-3451.	2.9	12
5	Ultrasensitive Analysis of Exosomes Using a 3D Self-Assembled Nanostructured SiO ₂ Microfluidic Chip. ACS Applied Materials & Interfaces, 2022, 14, 14693-14702.	4.0	18
6	Fc-MBL-modified Fe3O4 magnetic bead enrichment and fixation in Gram stain for rapid detection of low-concentration bacteria. Mikrochimica Acta, 2022, 189, 169.	2.5	1
7	Protein FT-IR amide bands are beneficial to bacterial typing. International Journal of Biological Macromolecules, 2022, 207, 358-364.	3.6	7
8	Progress in infrared spectroscopy as an efficient tool for predicting protein secondary structure. International Journal of Biological Macromolecules, 2022, 206, 175-187.	3.6	64
9	The chirality determination of amino acids by forming complexes with cyclodextrins and metal ions using ion mobility spectrometry, and a DFT calculation. Talanta, 2022, 243, 123363.	2.9	14
10	MALDI-TOF MS method for differentiation of methicillin-sensitive and methicillin-resistant Staphylococcus aureus using (E)-Propyl α-cyano-4-Hydroxyl cinnamylate. Talanta, 2022, 244, 123405.	2.9	5
11	Efficient Classification of Escherichia coli and Shigella using FT-IR Spectroscopy and Multivariate Analysis. Spectrochimica Acta - Part A: Molecular and Biomolecular Spectroscopy, 2022, , 121369.	2.0	2
12	Simultaneous enrichment and analysis of benzimidazole by in-tube SPME-MS based on poly (3-Acrylamidophenylboronic acid-co-divinylbenzene-co-N,N′-methylenebisacrylamide) monolithic column. Talanta, 2021, 224, 121402.	2.9	5
13	Releasing bacteria from functional magnetic beads is beneficial to MALDI-TOF MS based identification. Talanta, 2021, 225, 121968.	2.9	11
14	4-Hydrazinoquinazoline acting as a reactive matrix for the rapid and sensitive analysis of neutral and sialylated glycans using MALDI MS. Analyst, The, 2021, 146, 6840-6845.	1.7	6
15	Discrimination of Aminobiphenyl Isomers in the Gas Phase and Investigation of Their Complex Conformations. Journal of the American Society for Mass Spectrometry, 2021, 32, 716-724.	1.2	6
16	Enantioâ€separation of pregabalin by ternary complexation using trapped ion mobility spectrometry. Rapid Communications in Mass Spectrometry, 2021, 35, e9052.	0.7	4
17	Mitochondrial Targeting Strategy for Enhanced Photothermal Cancer Therapy. ChemNanoMat, 2021, 7, 457-466.	1.5	2
18	CaCO ₃ -Encapsulated Au Nanoparticles Modulate Macrophages toward M1-like Phenotype. ACS Applied Bio Materials, 2021, 4, 3214-3223.	2.3	10

#	Article	IF	CITATIONS
19	Novel Facile Oneâ€Pot Synthesis of Bi ₂ S ₃ â^BiOCl Ultrathin Heteroâ€nanosheets for Selective Alcohol Oxidation. ChemCatChem, 2021, 13, 2293-2302.	1.8	11
20	Application of MALDI-TOF MS Profiling Coupled With Functionalized Magnetic Enrichment for Rapid Identification of Pathogens in a Patient With Open Fracture. Frontiers in Chemistry, 2021, 9, 672744.	1.8	5
21	Direct distinction of ibuprofen and flurbiprofen enantiomers by ion mobility mass spectrometry of their ternary complexes with metal cations and cyclodextrins in the gas phase. Journal of Separation Science, 2021, 44, 2474-2482.	1.3	11
22	Direct and simultaneous recognition of the positional isomers of aminobenzenesulfonic acid by TIMS-TOF-MS. Talanta, 2021, 226, 122085.	2.9	9
23	Rapid and specific detection nanoplatform of serum exosomes for prostate cancer diagnosis. Mikrochimica Acta, 2021, 188, 283.	2.5	14
24	Rapid identification of bacteria directly from blood cultures by Co-magnetic bead enrichment and MALDI-TOF MS profiling. Talanta, 2021, 233, 122472.	2.9	6
25	Evolution of the protein corona affects macrophage polarization. International Journal of Biological Macromolecules, 2021, 191, 192-200.	3.6	9
26	Effective discrimination of Yersinia pestis and Yersinia pseudotuberculosis by MALDI-TOF MS using multivariate analysis. Talanta, 2021, 234, 122640.	2.9	1
27	The strategy for correcting interference from water in Fourier transform infrared spectrum based bacterial typing. Talanta, 2020, 208, 120347.	2.9	19
28	Evaluation of prostate cancer based on MALDI-TOF MS fingerprinting of nanoparticle-treated serum proteins/peptides. Talanta, 2020, 220, 121331.	2.9	10
29	Labeled-protein corona-coated Bi2S3 nanorods targeted to lysosomes for bioimaging and efficient photothermal cancer therapy. Colloids and Surfaces B: Biointerfaces, 2020, 196, 111291.	2.5	11
30	Microfluidic Raman biochip detection of exosomes: a promising tool for prostate cancer diagnosis. Lab on A Chip, 2020, 20, 4632-4637.	3.1	80
31	Quantifying Nonâ€Covalent Binding Interactions between Tobacco Alkaloids and Cyclodextrin Using Mass Spectrometry and the Application in Cigarette Smoke. ChemistrySelect, 2020, 5, 6658-6665.	0.7	1
32	FTIR-assisted MALDI-TOF MS for the identification and typing of bacteria. Analytica Chimica Acta, 2020, 1111, 75-82.	2.6	37
33	Cross-Linked Polyamide Chains Enhanced the Fluorescence of Polymer Carbon Dots. ACS Omega, 2020, 5, 8219-8229.	1.6	9
34	SERS-based immunocapture and detection of pathogenic bacteria using aÂboronic acid-functionalized polydopamine-coated Au@Ag nanoprobe. Mikrochimica Acta, 2020, 187, 290.	2.5	20
35	Thuricinâ€Z: A Narrow‧pectrum Sactibiotic that Targets the Cell Membrane. Angewandte Chemie - International Edition, 2019, 58, 18793-18797.	7.2	42
36	Conformational-transited protein corona regulated cell-membrane penetration and induced cytotoxicity of ultrasmall Au nanoparticles. RSC Advances, 2019, 9, 4435-4444.	1.7	23

#	Article	IF	CITATIONS
37	Detailed insight into the formation of protein corona: Conformational change, stability and aggregation. International Journal of Biological Macromolecules, 2019, 135, 1114-1122.	3.6	18
38	Protein Binding on the Surface of Magnetic Nanoparticles. Particle and Particle Systems Characterization, 2019, 36, 1900072.	1.2	4
39	Movements of the Substrate-Binding Clamp of Cypemycin Decarboxylase CypD. Journal of Chemical Information and Modeling, 2019, 59, 2924-2929.	2.5	7
40	Convergent evolution of the Cys decarboxylases involved in aminovinyl ysteine (AviCys) biosynthesis. FEBS Letters, 2019, 593, 573-580.	1.3	23
41	Fluorescent polymer dots and graphene oxide based nanocomplexes for "off-on―detection of metalloproteinase-9. Nanoscale, 2019, 11, 20903-20909.	2.8	17
42	The Competitive Dynamic Binding of Some Blood Proteins Adsorbed on Gold Nanoparticles. Particle and Particle Systems Characterization, 2019, 36, 1800257.	1.2	19
43	Identification of pathogenic bacteria in human blood using IgG-modified Fe3O4 magnetic beads as a sorbent and MALDI-TOF MS for profiling. Mikrochimica Acta, 2018, 185, 542.	2.5	33
44	Biosynthetic Insights into Linaridin Natural Products from Genome Mining and Precursor Peptide Mutagenesis. ACS Chemical Biology, 2017, 12, 1484-1488.	1.6	31
45	Solid-film sampling method for the determination of protein secondary structure by Fourier transform infrared spectroscopy. Analytical and Bioanalytical Chemistry, 2017, 409, 4459-4465.	1.9	17
46	Probing the binding affinity of plasma proteins adsorbed on Au nanoparticles. Nanoscale, 2017, 9, 4787-4792.	2.8	77
47	Probing the mechanism of plasma protein adsorption on Au and Ag nanoparticles with FT-IR spectroscopy. Nanoscale, 2015, 7, 15191-15196.	2.8	63
48	Obtaining information about protein secondary structures in aqueous solution using Fourier transform IR spectroscopy. Nature Protocols, 2015, 10, 382-396.	5.5	819
49	Serum albumin adsorbed on Au nanoparticles: structural changes over time induced by S–Au interaction. Chemical Communications, 2015, 51, 3634-3636.	2.2	33
50	Binding of calmodulin changes the calcineurin regulatory region to a less dynamic conformation. International Journal of Biological Macromolecules, 2015, 79, 235-239.	3.6	6
51	Probing the Ca2+/CaM-induced secondary structural and conformational changes in calcineurin. International Journal of Biological Macromolecules, 2014, 64, 453-457.	3.6	11
52	Calcium-dependent conformational transition of calmodulin determined by Fourier transform infrared spectroscopy. International Journal of Biological Macromolecules, 2013, 56, 57-61.	3.6	6
53	Effects of activating cations and inhibitor on the allosteric regulation of rabbit muscle pyruvate kinase. International Journal of Biological Macromolecules, 2013, 60, 219-225.	3.6	0
54	Structural dynamic and thermodynamic analysis of calcineurin B subunit induced by calcium/magnesium binding. International Journal of Biological Macromolecules, 2013, 60, 122-127.	3.6	2

#	Article	IF	CITATIONS
55	Overestimated accuracy of circular dichroism in determining protein secondary structure. European Biophysics Journal, 2013, 42, 455-461.	1.2	8
56	The N-terminal Capping Propensities of the D-helix Modulate the Allosteric Activation of the Escherichia coli cAMP Receptor Protein. Journal of Biological Chemistry, 2012, 287, 39402-39411.	1.6	13
57	Roles of hinge region, loops 3 and 4 in the activation of Escherichia coli cyclic AMP receptor protein. International Journal of Biological Macromolecules, 2012, 50, 1-6.	3.6	8
58	Calcium-induced changes in calmodulin structural dynamics and thermodynamics. International Journal of Biological Macromolecules, 2012, 50, 1011-1017.	3.6	33
59	Probing the catalytic allosteric mechanism of rabbit muscle pyruvate kinase by tryptophan fluorescence quenching. European Biophysics Journal, 2012, 41, 607-614.	1.2	4
60	The conformational change of rabbit muscle pyruvate kinase induced by activating cations and its substrates. International Journal of Biological Macromolecules, 2010, 47, 228-232.	3.6	6
61	The role of loops 3 and 4 in the interdomains and intersubunits communication of E. coli cAMP receptor protein. International Journal of Biological Macromolecules, 2008, 42, 372-379.	3.6	5
62	The Secondary Structure of Calcineurin Regulatory Region and Conformational Change Induced by Calcium/Calmodulin Binding. Journal of Biological Chemistry, 2008, 283, 11407-11413.	1.6	34
63	Fourier Transform Infrared Spectroscopic Analysis of Protein Secondary Structures. Acta Biochimica Et Biophysica Sinica, 2007, 39, 549-559.	0.9	2,565
64	Dissecting the Mechanism of Epac Activation via Hydrogenâ^'Deuterium Exchange FT-IR and Structural Modelingâ€. Biochemistry, 2006, 45, 15318-15326.	1.2	35
65	Probing cAMP-Dependent Protein Kinase Holoenzyme Complexes Iα and IIβ by FT-IR and Chemical Protein Footprinting. Biochemistry, 2004, 43, 1908-1920.	1.2	14
66	Role of Residue 138 in the Interdomain Hinge Region in Transmitting Allosteric Signals for DNA Binding inEscherichia colicAMP Receptor Proteinâ€. Biochemistry, 2004, 43, 4662-4669.	1.2	26
67	Solution Structure and Structural Dynamics of Envelope Protein Domain III of Mosquito- and Tick-Borne Flavivirusesâ€. Biochemistry, 2004, 43, 9168-9176.	1.2	38
68	Effects of metabolites on the structural dynamics of rabbit muscle pyruvate kinase. Biophysical Chemistry, 2003, 103, 1-11.	1.5	21